Electronic Supplementary Material (ESI) for Journal of Materials Chemistry A.

Supporting Information

Green synthesis of polypyrrole tubes using curcumin template for excellent electrochemical performance in supercapacitors

Jincy Parayangattil Jyothibasu[a,b] and Rong-Ho Lee[*a]

[a]Department of Chemical Engineering, National Chung Hsing University, Taichung 402, Taiwan

[b]Department of Environmental Engineering, National Chung Hsing University, Taichung 402, Taiwan

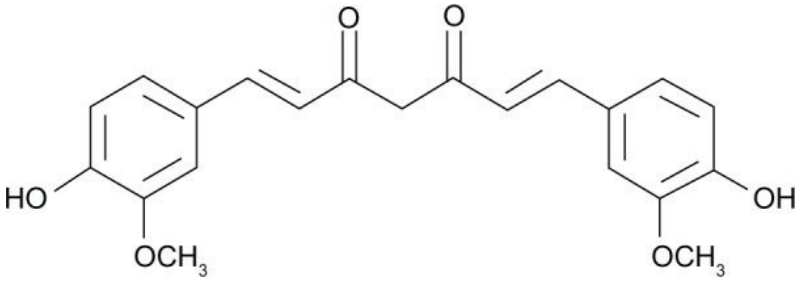

Fig. S1 Chemical structure of curcumin.

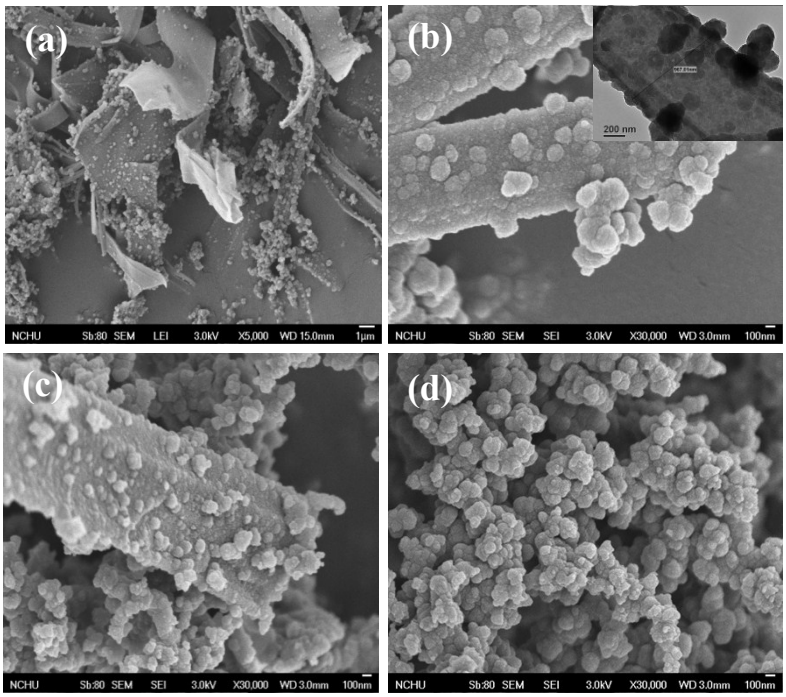

Fig. S2 (a) SEM image of PPyC1T1. (b, c) High-magnification SEM images of (b) PPyC1T2 and (c) PPyC1T4. (d) SEM image of PPy nanoparticles synthesized in the absence of the template. Inset to (b): TEM image of PPyC1T2.

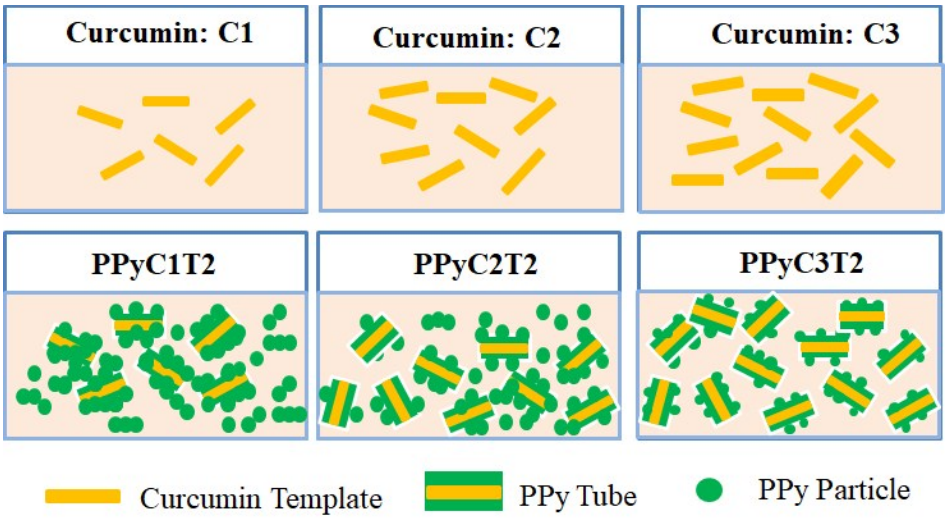

Fig. S3 Schematic representation of the mechanism of formation of tubular PPy (PPyT) at various concentrations of curcumin.

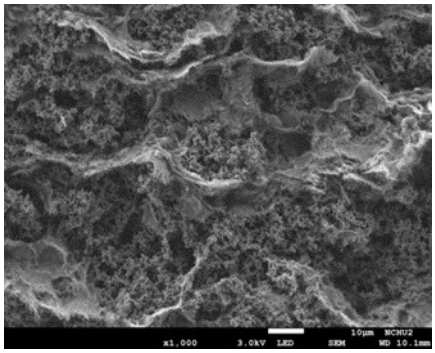

Fig. S4 SEM image of the PPy nanoparticle/*f*-CNT composite film.

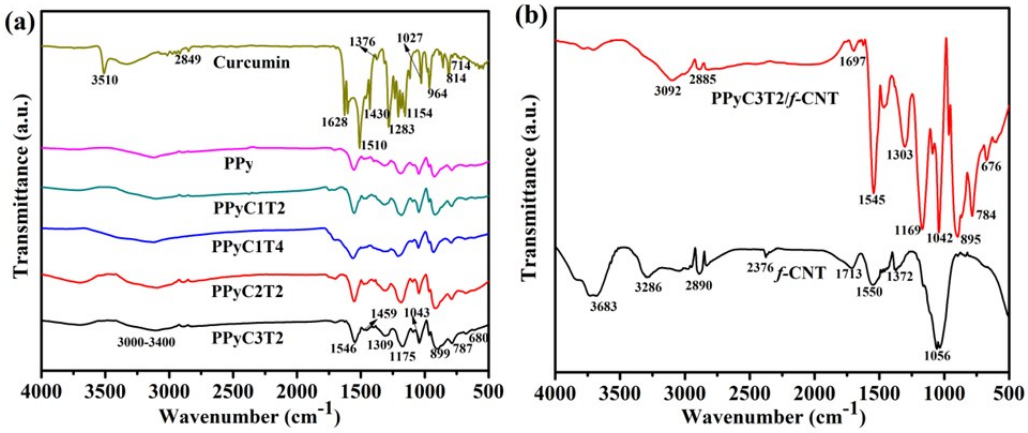

Fig. S5 FTIR spectra of (a) curcumin, PPy, PPyC1T2, PPyC1T4, PPyC2T2, and PPyC3T2 and (b) the *f*-CNTs and the PPyC3T2/*f*-CNT composite.

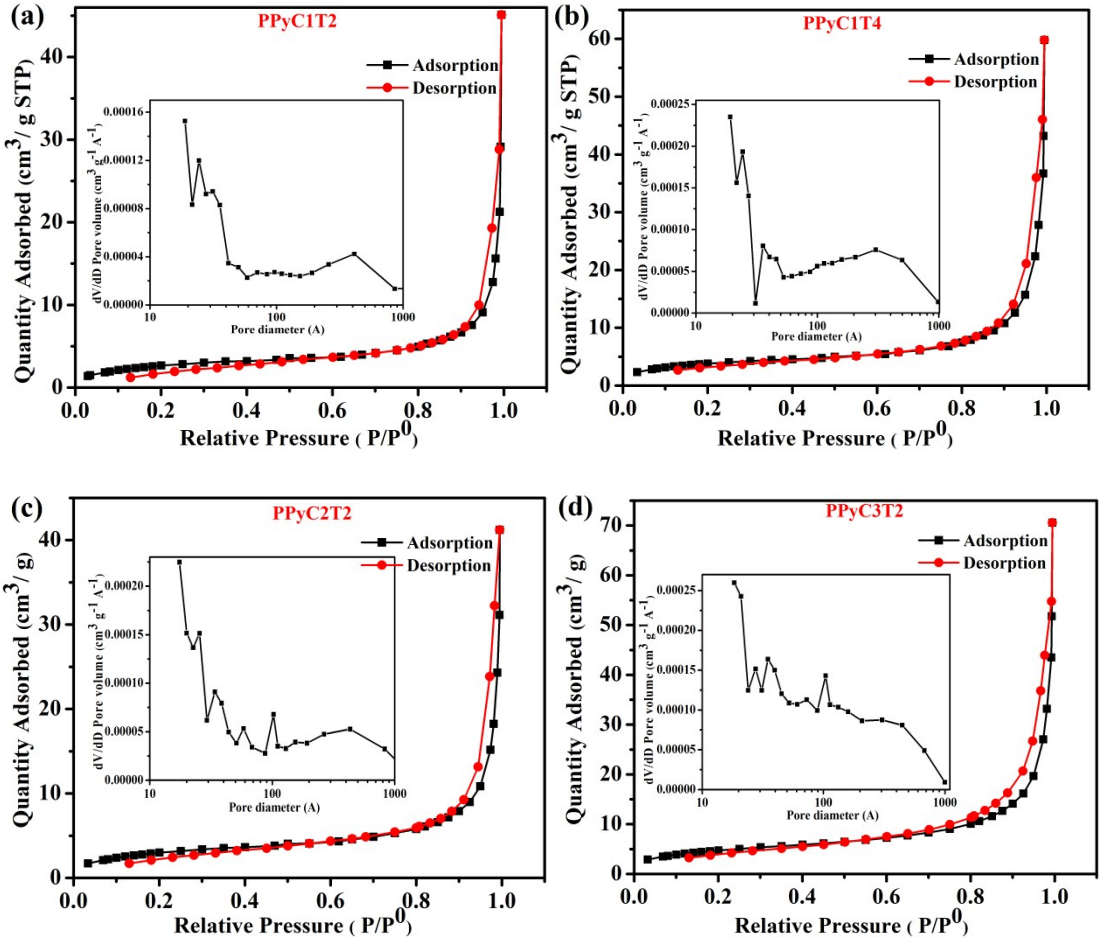

Fig. S6 Nitrogen adsorption/desorption isotherms of PPyC1T2, PPyC1T4, PPyC2T2, and PPyC3T2; insets: corresponding pore size distribution curves.

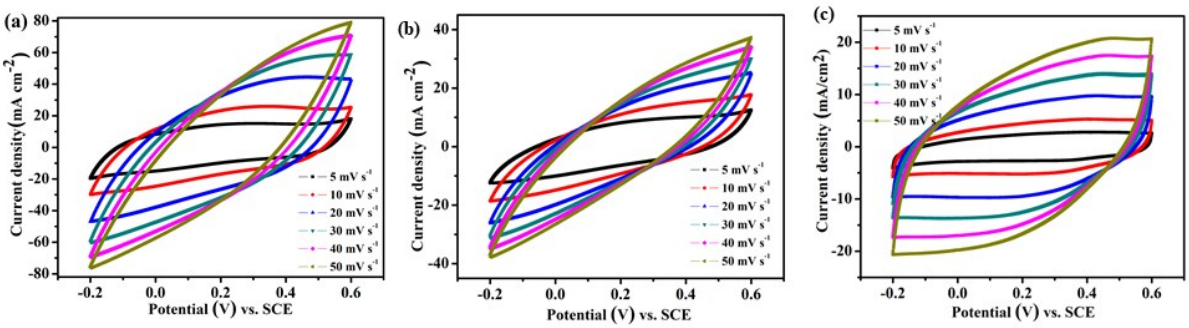

Fig. S7 CV curves, recorded at scan rates from 5 to 50 mV s^{-1}, of (a) the PPyC1T2/*f*-CNT freestanding electrode, (b) the PPyC1T4/*f*-CNT freestanding electrode, and (c) the *f*-CNT freestanding electrode.

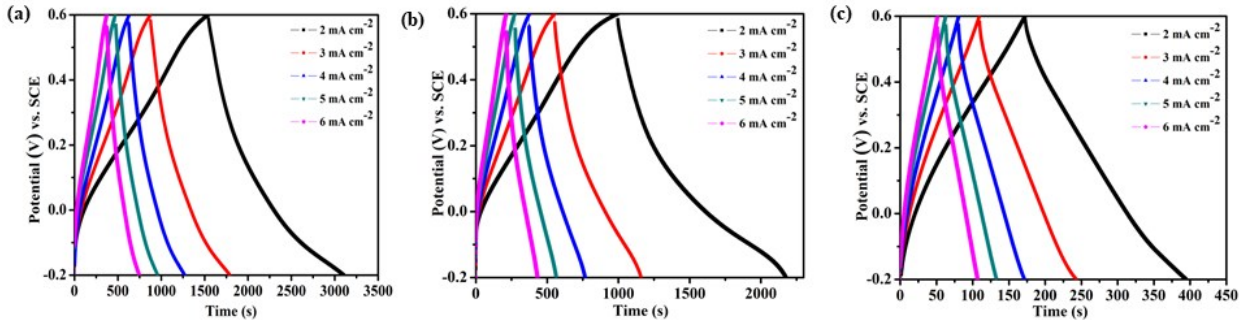

Fig. S8 GCD curves, recorded at current densities from 2 to 6 mA cm^{-2}, of the (a) PPyC1T2/*f*-CNT, (b) PPyC1T4/*f*-CNT, and (c) *f*-CNT freestanding electrodes.

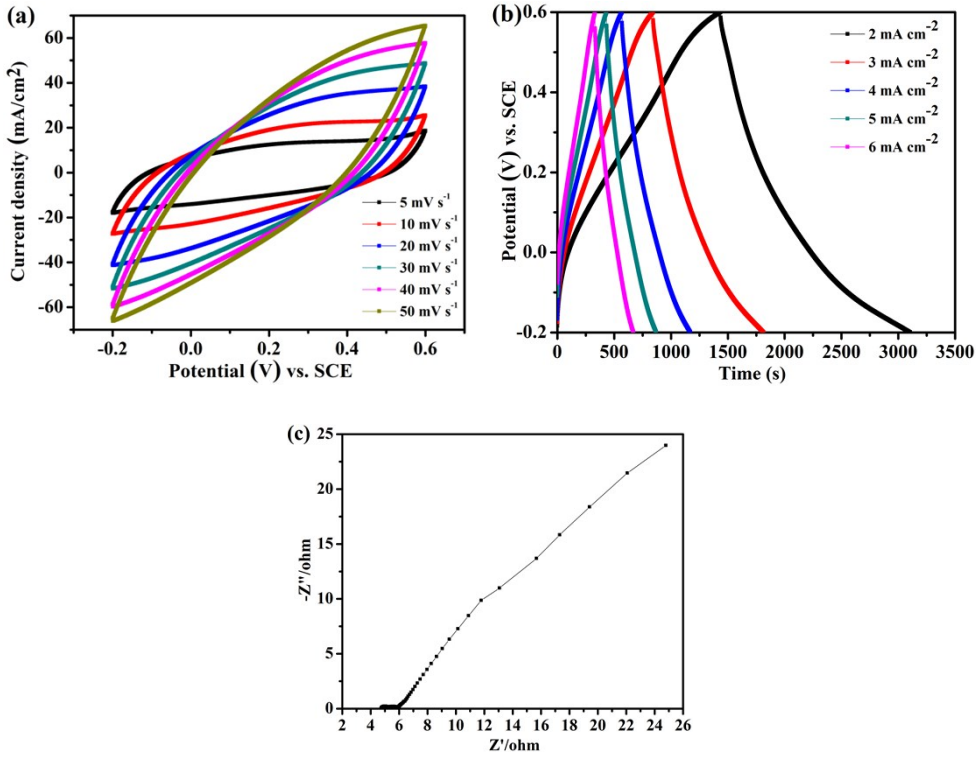

Fig. S9 Electrochemical performance of the PPy nanoparticle/*f*-CNT freestanding electrode in a three-electrode system. (a) CV curves recorded at a scan rate of 5 mV s^{-1}. (b) GCD curves recorded at a current density of 2 mA cm^{-2}. (c) Nyquist plots determined using EIS.

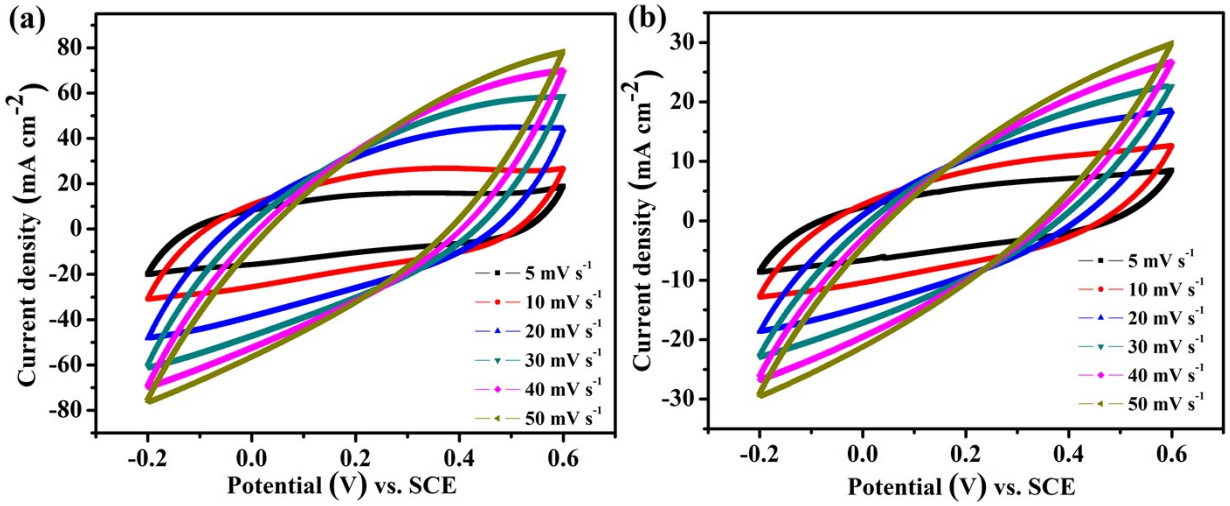

Fig. S10 CV curves, recorded at scan rates from 5 to 50 mV s^{-1}, of the (a) PPyC2T2/*f*-CNT and (b) PPyC3T2 freestanding electrodes.

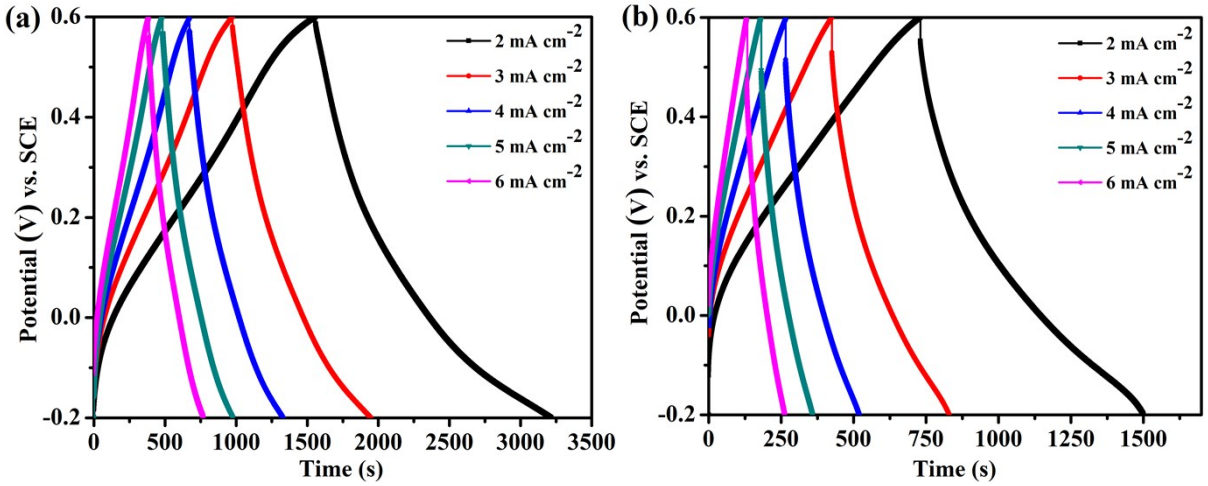

Fig. S11 GCD curves, recorded at current densities from 2 to 6 mA cm^{-2}, of the (a) PPyC2T2/*f*-CNT and (b) PPyC3T2 freestanding electrodes.

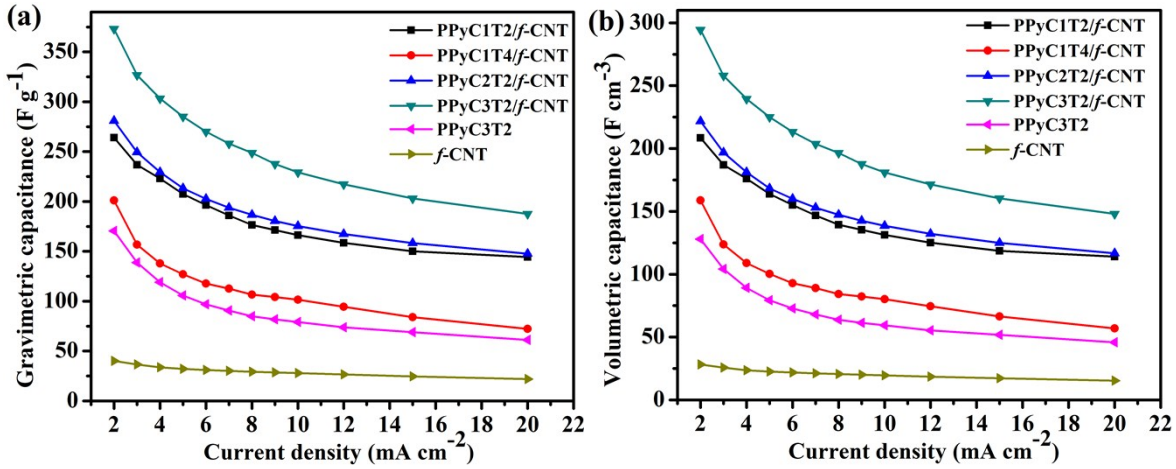

Fig. S12 (a) Gravimetric and (b) volumetric capacitances of the PPyC1T2/*f*-CNT, PPyC1T4/*f*-CNT, PPyC2T2/*f*-CNT, PPyC3T2/*f*-CNT, PPyC3T2, and *f*-CNT freestanding electrodes, plotted with respect to the current density.

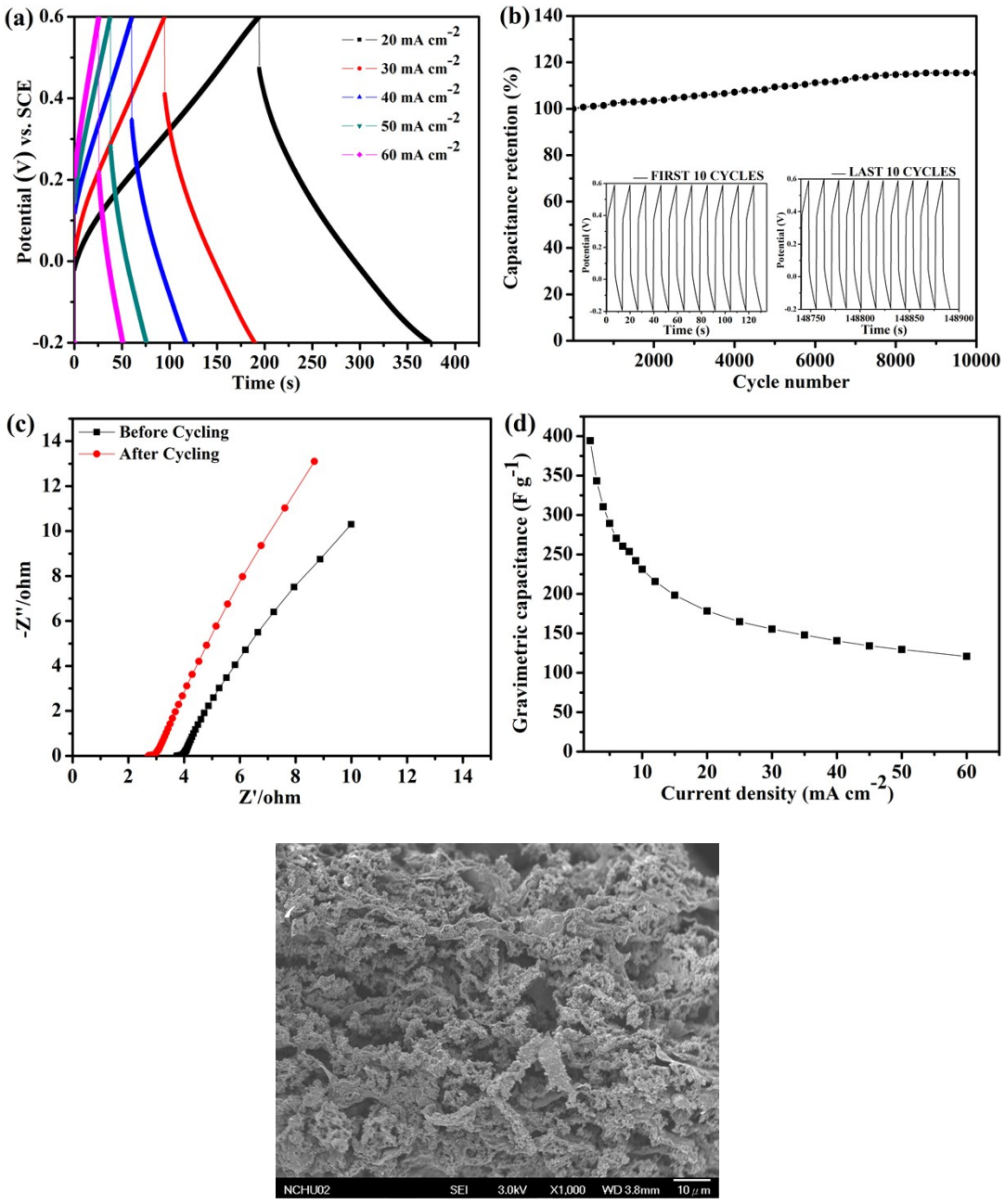

Fig. S13 Electrochemical performance of the PPyC3T2/*f*-CNT-thick freestanding electrode having a high mass loading of 30 mg cm^{-2}, measured in a three-electrode system. (a) GCD curves recorded at current densities from 20 to 60 mA cm^{-2}. (b) Cyclic performance recorded at a high current density of 90 mA cm^{-2} for 10,000 charge/discharge cycles. (c) EIS spectra recorded before and after the cycling life test. (d) Gravimetric capacitances plotted with respect to the current density. (e) SEM image of PPyC3T2/*f*-CNT-thick freestanding electrode after cycling test.

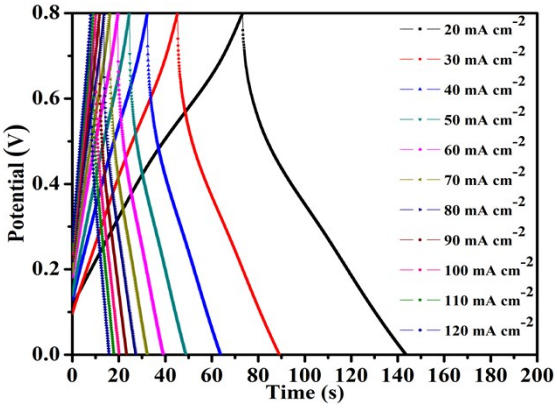

Fig. S14 GCD curves recorded at higher current densities, from 20 to 120 mA cm^{-2}, for the symmetric supercapacitor incorporating PPyC3T2/*f*-CNT-thick freestanding electrodes.

Table S1 Capacitive performances of conducting polymer-based composite electrodes reported previously in the literature and in this present paper

Electrode materials	Active material loading	Current collector	Areal capacitance of electrode (C_A)	Reference
PPy tubes/*f*-CNTs	30.0 mg cm^{-2}	Freestanding electrode without current collector	11,830.4 mF cm^{-2} (295.8 F cm^{-3}) (394.4 F g^{-1}) at a current density of 2 mA cm^{-2}	This study
PPy-coated CNT paper	12.1 mg cm^{-2}	Freestanding electrode	8604.5 mF cm^{-2} at a current density of 1 mA cm^{-2}	*J. Mater. Chem. A*, 2019, **7**, 10751–10760
Tiron-doped PPy/MWCNT composite electrode	27 mg cm^{-2}	Ni foam	7.8 F cm^{-2} at a scan rate of 0.5 mV s^{-1}	*J. Appl. Polym. Sci.*, 2015, **132**, 42376.
PPy hydrogel	20 mg cm^{-2}	Carbon cloth	6.4 F cm^{-2} at a current density of 0.14 A g^{-1}	*J. Mater. Chem. A*, 2014, **2**, 6086–6091
Porous polyaniline/reduced graphene oxide composite material	7.1 mg cm^{-2}	Freestanding electrode	5830 mF cm^{-2} at a current density of 15.72 mA cm^{-2} (824 F g^{-1} at 2.22 A g^{-1})	*Energy Environ. Sci.*, 2018, **11**, 1280–1286
Nanostructured PPy/ MWCNT networks on cotton fabrics	–	Freestanding electrode	5.05 F cm^{-2} at a scan rate of 1 mV s^{-1}	*Cellulose*, 2019, **26**, 4071–4084.
PPy-coated CNTs	18 mg cm^{-2}	Ni foam	4.798 F cm^{-2} at a scan rate of 2 mV s^{-1}	*J. Mater. Chem. A*, 2014, **2**, 14666–14673
PPy-coated air-laid paper	–	Freestanding electrode	3100 mF cm^{-2} at a current density of 1	*Adv. Energy Mater.*, 2017, **7**,

			mA cm^{-2}	1701247
PPy nanofiber–MWCNT electrodes	30 mg cm^{-2}	Ni foam	4.62 F cm^{-2} at a scan rate of 2 mV s^{-1}	*J. Mater. Chem. A*, 2013, **1**, 11614–11622
PPy-coated knitted fabric	12.3 mg cm^{-2}	Freestanding electrode	4117 mF cm^{-2} at a current density of 2 mA cm^{-2}	*J. Mater. Chem. A*, 2016, **4**, 12981–12986
Cellulose nanofiber/cellulose-derived carbon sheet/ polyaniline nanocomposite film	–	Freestanding electrode	3297.2 mF cm^{-2} (220 F g^{-1}) at a current density of 1 mA cm^{-2}	*J. Mater. Chem. A*, 2016, **4**, 13352–13362
Polypyrrole/nylon membrane composite film	5 mg cm^{-2}	Freestanding electrode	2911.4 mF cm^{-2} at a current density of 1 mA cm^{-2}	*J. Materiomics,* 2019, DOI: https://doi.org/10.1016/j.jmat.2019.11.004.
Microfibrillated cellulose fiber (MCF) framework/ chitosan-derived N-self-doped carbon sheet (N-CS)/PANI composite electrode	–	Freestanding electrode	1688.8 mF cm^{-2} (139.6 F g^{-1}, 84.4 F cm^{-3}) at a current density of 1 mA cm^{-2}	*J. Mater. Chem. A*, 2018, **6**, 20338–20346
PANI/CNT/air-laid paper composite electrode	3.32 mg cm^{-2}	Freestanding electrode	1506 mF cm^{-2} at a current density of 10 mA cm^{-2}	*J. Mater. Chem. A*, 2017, **5**, 19934–19942
PPy-coated cotton fabrics	5.7 mg cm^{-2}	Freestanding electrode	1325 mF cm^{-2} at 2 mA cm^{-2}	*RSC Adv*., 2017, **7**, 48934–48941
PPy/paper composite electrode	3.54 mg cm^{-2}	Freestanding electrode	1.5 F cm^{-2} at 1 mA cm^{-2}	*Energy Environ. Sci*., 2013, **6**, 470–476
Polypyrrole on vertically aligned carbon nanotube arrays/carbon fiber paper	0.84 mg cm^{-2}	Carbon fiber paper	0.78 F cm^{-2} at 2 mV s^{-1}	*J. Mater. Chem. A*, 2015, **3**, 22043–22052

(PPy/VA-CNTs/CFP)				
Polyaniline/carbon nanotubes/graphene/polyester textile electrode	–	Freestanding electrode	791 mF cm^{-2} at a current density of 1.5 mA cm^{-2}	*Electrochim. Acta*, 2017, **249**, 387–394
Carbon nanotube/polyaniline hydrogel film	–	Freestanding electrode	680 mF cm^{-2} at 1 mA cm^{-2}	*J. Mater. Chem. A*, 2015, **3**, 23864–23870
PEDOT nanowire film	–	Freestanding electrode	667.5 mF cm^{-2} at 1 mA cm^{-2}	*J. Mater. Chem. A*, 2019, **7**, 1323–1333
rGO/PPy NT paper	2.46 mg cm^{-2}	Carbon paper	807 mF cm^{-2} at 1 mA cm^{-2}	*J. Power Sources*, 2016, **302**, 39–45
Graphene/activated carbon/polypyrrole (GN/AC/PPy)	2.75 mg cm^{-2}	Freestanding electrode	906 mF cm^{-2} at a current density of 0.5 mA cm^{-2}	*RSC Adv.*, 2017, **7**, 31342–31351
Free-standing reduced graphene oxide/polypyrrole/cellulose hybrid papers	–	Freestanding electrode	1.20 F cm^{-2} at 2 mA cm^{-2}	*J. Mater. Chem. A*, 2017, **5**, 3819–3831
CuO NWAs@PEDOT:PSS composite electrode	–	Cu foam	907.5 mF cm^{-2} at 3 mA cm^{-2}	*J. Mater. Sci.: Mater. Electron.*, 2019, **30**, 10953–10960
PEDOT/CC hybrid electrode	–	Carbon cloth	201.4 mF cm^{-2} at 1 mA cm^{-2}	*Nanotechnology*, 2016, **27**, 385705
rGO-PEDOT/PSS film	8.49 mg cm^{-2}	Freestanding electrode	448 mF cm^{-2} at a scan rate of 10 mV s^{-1}	*Sci. Rep.*, 2015, **5**, 17045